Influence of Adding Unfunctionalized PEO on the Viscoelasticity and the Structure of Dense Polymeric Micelle Solutions Formed by Hydrophobically End-Capped PEO

Frédéric Renou, Lazhar Benyahia, and Taco Nicolai*

Polymères, colloïdes, Interfaces, UMR CNRS 6120, Université du Maine, 72085 Le Mans Cedex 9, France

Received January 30, 2007; Revised Manuscript Received April 5, 2007

ABSTRACT: Hydrophobically end-capped poly(ethylene oxide) (PEO) is a highly asymmetric diblock copolymer that forms spherical micelles in water resembling multiarm star polymers. The dynamic mechanical properties of these polymeric micelles were studied in the absence and in the presence of unfunctionalized PEO chains as a function of concentration and temperature. A discontinuous reversible liquid−solid transition was observed below a critical temperature (T_c). Addition of linear chains led to a decrease of T_c and a strong slowing down of the kinetics of the transition close to T_c. Flow measurements of the solid showed a steep power law decrease of the flow rate with decreasing stress. For a given stress the flow rate increased after addition of linear chains, but the stress dependence of the flow rate remained the same. Dynamic and static light scattering measurements were done to investigate the influence of adding linear chains on the osmotic compressibility and the cooperative diffusion of polymeric micelle solutions.

Introduction

Polymeric micelles are formed in solution by asymmetric diblock copolymers through the association of small insoluble groups grafted at one end of soluble polymer chains.[1] These micelles may be considered as star polymers with the important difference that the number of arms (p) can vary as a function of concentration or temperature. It is important to distinguish between dynamic polymeric micelles that can rapidly exchange arms and frozen micelles for which the exchange is very slow or even absent.[2] Only the former can adapt to changes of the concentration and the temperature by varying p and thus the number of micelles. The latter resemble more closely covalently bonded star polymers.

Solutions of multiarm star polymers[3,4] or polymeric micelles[1] may stop flowing freely above a critical volume fraction because the micelles are jammed. Jammed micelle solutions have sometimes been called gels, but since there is no bond formation between the micelles, we prefer to call them solids. Of course, the PEO segments remain mobile when the micelles are jammed. The relevant parameter for the liquid−solid transition is the effective thermodynamic volume fraction of the micelles. Therefore, the transition can also be obtained by varying the temperature in marginal solvents. For polymeric micelles the transition is invariably accompanied by crystalline ordering of the micelles. Even though the elastic mechanical response is sometimes explained in terms of the crystal order,[5] the latter is not necessary for the liquid−solid transition. It was recently shown for polymeric micelles based on hydrophobically end-capped poly(ethylene oxide) (PEO) that a disordered solid is formed first and that the crystalline order appears more slowly.[6] In addition, covalently bound star polymers show a liquid−solid transition, but usually no crystal order.[7] The liquid−solid transition may thus be considered as a glass transition.

For star polymers in athermal solvents the phase diagram[8] and the glass transition[9] have been described theoretically.[10] The predictions were confirmed in part by experiments on frozen polymeric micelles.[11] A different interaction potential has been used to describe the interaction of star polymers in marginal solvents.[12] Theory and computer simulations indicate that crystallization and glass formation occur at approximately the same volume fraction both in athermal and marginal solvents.[9,13]

It has been reported[14] that addition of linear homopolymers to polymeric micelles leads to melting of the solid and disruption of the crystal order. More recently, the same effect was reported for covalent star polymers.[15] Addition of linear chains to star polymers decreased the shear moduli of the solid and induced melting above a critical fraction of linear chains. The effect increased with increasing molar mass of the linear chains and was attributed to depletion effects or shrinking of the star polymers. The effect disappeared for chains much smaller than the star arms, while for chains much larger than the arms an effect of bridging was observed. Yamazaki et al.[16,17] observed the same phenomena when adding linear PEO to small polymeric micelles formed by hydrophobically modified PEO.

The aim of the work presented here was to investigate in more detail the dramatic effect of adding linear chains on the liquid−solid transition and the flow behavior of polymeric micelle solutions. We studied the rheology of mixtures of polymeric micelles formed by alkyl end-capped PEO and linear PEO with same molar mass (4.3×10^3 g/mol). The functionalized PEO formed spherical micelles in dilute aqueous solutions with $p = 32$ independent of the temperature. We also investigated the effect of adding linear chains on the amplitude and relaxation of spontaneous concentration fluctuations in the micelle solutions using static and dynamic light scattering. A detailed study of structural and mechanical properties of the PEO micelles in the absence of linear chains has been reported earlier.[6,18]

Experimental Section

Materials. PEO end-capped with octadecyl (Brij 700, batch 05214MC) and nonfunctionalized PEO were purchased from Aldrich. We tested several batches and observed small differences

* Corresponding author. E-mail: Taco.Nicolai@univ-lemans.fr.

10.1021/ma070263e CCC: $37.00
Published on Web 05/27/2007

in the critical concentration for gelation. On the basis of the results presented here, we can explain these differences by the presence of a small weight fraction (<5%) of nonfunctionalized PEO in varying quantities. We have chosen the batch with the lowest critical concentration of gelation and consequently the lowest fraction of nonfunctionalized chains. The weight-average molar mass, M_w = 4.3 kg/mol, and the polydispersity index, $M_w/M_n = 1.05$, were the same for both polymers. Clear solutions in pure "Millipore" water were obtained after stirring for an hour at 80 °C. The total PEO concentrations (C) were calculated using a density of 1.15 kg/L.[19] The small temperature dependence of the density was ignored. At concentrations above 750 g/L both functionalized and nonfunctionalized PEO were no longer soluble and crystallized at room temperature. The crystallization of PEO segments at very high concentrations should not be confused with the crystalline order of the micelles at much lower PEO concentrations. In the latter case the PEO segments are hydrated and mobile.

Mixtures with different weight fractions of linear nonfunctionalized PEO chains with respect to the total mass of PEO (F) were prepared by mixing aqueous solutions of the pure systems at 80 °C. Transparent homogeneous solutions were obtained in all cases. For light scattering measurements the samples were filtered through 0.2 μm pore size Anatop filters when it was possible, while more viscous samples were filtered through 0.45 μm pore size filters. Highly viscous solutions obtained at the highest concentrations could not be filtered but were purified by ultracentrifugation. We verified that filtration or centrifugation did not modify the PEO concentration.

Rheology. Rheology measurements were done on a stress-controlled rheometer (AR1000, TA Instruments) using a cone and plate geometry (diameter 6 cm and angle 0.58° or 4 cm and 2°). The temperature was controlled using a Peltier system. Solvent evaporation was avoided by covering the geometry with mineral oil. Oscillatory measurements were done at 1 Hz with an imposed stress of 10 Pa or an imposed deformation of 0.5% to determine the storage (G') and loss modulus (G''). In both cases the measurements were in the linear response regime for the solids and the liquids. However, only in the case of imposed deformation was the response linear during the transition. Nevertheless, the results were close, and here only the results using imposed stress are shown because they contain less noise. For the liquid the dynamic viscosity obtained from G'' was the same as the viscosity obtained from flow measurements with an imposed stress of 10 Pa.

Light Scattering. Light scattering measurements were made using an ALV-5000 multibit, multitau, full digital correlator in combination with a Spectra-Physics laser emitting vertically polarized light at $\lambda = 532$ nm. The temperature was controlled by a thermostat bath to within ±0.1 °C. The relative excess scattering intensity (I_r) was determined as the total intensity minus the solvent scattering divided by the scattering of toluene at 20 °C. I_r is related to the osmotic compressibility ($(d\pi/dC)^{-1}$) and the z-average structure factor ($S(q)$):[20,21]

$$I_r = KCRT(d\pi/dC)^{-1}S(q) \tag{1}$$

with R the gas constant and T the absolute temperature.

$$K = \frac{4\pi^2 n^2}{\lambda^4 N_a}\left(\frac{dn}{dC}\right)^2\left(\frac{n_s}{n}\right)^2\frac{1}{R_s} \tag{2}$$

where N_a is Avogadro's number, λ is the wavelength of the incident light, dn/dC is the refractive index increment, and R_s is the Rayleigh ratio of toluene. $(n_s/n)^2$ corrects for the difference in scattering volume of the solution with refractive index n and toluene with refractive index n_s. $S(q)$ describes the dependence of I_r on the scattering wave vector: $q = (4\pi n/\lambda)\sin(\theta/2)$, with θ the angle of observation. $R_s = 2.79 \times 10^{-5}$ cm $^{-1}$ at $\lambda = 532$ nm and 20 °C. The refractive index increment of PEO is 0.135 cm^3/g,[22,23] and we have assumed that the value for functionalized PEO is the same because the functional group is small. In dilute solutions the osmotic compressibility may be written in terms of a virial expansion:

$$\frac{d\pi}{dC} = RT\left(\frac{1}{M_w} + 2A_2C + 3A_3C^2...\right) \tag{3}$$

where M_w is the weight-average molar mass and A_2 and A_3 are the second and third virial coefficients.

The normalized electric field autocorrelation function, $g_1(t)$, was calculated from the measured intensity correlation function using the so-called Siegert relation.[24] $g_1(t)$ was analyzed in terms of a relaxation time (τ) distribution using the REPES routine:[25]

$$g_1(t) = \int A(\tau)\exp(-t/\tau)\,d\tau \tag{4}$$

For all systems a fast q^2-dependent relaxation mode was observed caused by the relaxation of the concentration fluctuations of the linear chains and micelles. The cooperative diffusion coefficient was calculated from the average relaxation rate as $D_c = \langle\tau^{-1}\rangle/q^2$.

In addition, a slow diffusional mode was observed caused by the presence of large spurious scatterers, probably PEO aggregates.[26−29] The weight fraction of the spurious scatterers was negligible, but the q-dependent relative amplitude in the relaxation time distribution could still be substantial, as it is equal to the relative scattering intensity. At low concentrations when the samples could be filtered through 0.2 μm pore filters, the relative intensity scattered by the spurious scatterers was very small. However, with increasing concentration the relative intensity of the spurious scattering increased for two reasons. First, the relative scattering intensity of the fast mode decreased with increasing PEO concentration, and second, it was more difficult to remove the spurious scatterers for the more viscous solutions formed at higher concentrations.

In all cases I_r was corrected for the contribution of the spurious scattering, which could be as much as 50% at the highest concentrations, by multiplying the total scattering intensity with the relative amplitude of the fast mode. After correction, I_r was found to be independent of q. For solid samples $g_1(t)$ does not fully relax spontaneously. These samples were slowly rotated, which artificially forces $g_1(t)$ to relax with a terminal relaxation time that is determined by the speed of rotation.

Results

The rheometer was loaded with solutions containing a range of micelle concentrations up to 750 g/L. The solutions were presheared at 90 °C (5 min at 300 s^{-1}) in order to fully homogenize the system. Then the temperature was reduced at a rate of 5 °C/min down to 5 °C, during which the viscosity was measured using continuous shear with an imposed stress of 10 Pa (see Figure 1a). The liquid−solid transition was easily observed by the abrupt divergence of the viscosity at a temperature that increased with increasing concentration. The transition could be reversed by heating, but the melting temperature was higher than the freezing temperature. At a rate of 5 °C/min, the melting and the freezing temperatures differed by 2 or 3 deg, but this difference increased with increasing cooling and heating rates.[6]

Dynamic oscillatory shear measurements were done in the same way using an imposed stress of 10 Pa at 1 Hz (see Figure 1b). During cooling, G' increased sharply until a value characteristic of the solid state was reached which increased weakly on further cooling. When the solid was heated, the system melted again at a slightly higher temperature. It was shown in ref 18 that the frequency dependence of G' and G'' in the solid state is small.

The same experiments were done after adding linear PEO with different weight fractions (F) of the total amount of PEO. Figure 2 shows the temperature dependence of the viscosity of different micellar solutions with $F = 0.1$. A strong increase of the hysteresis between freezing and melting was observed, which

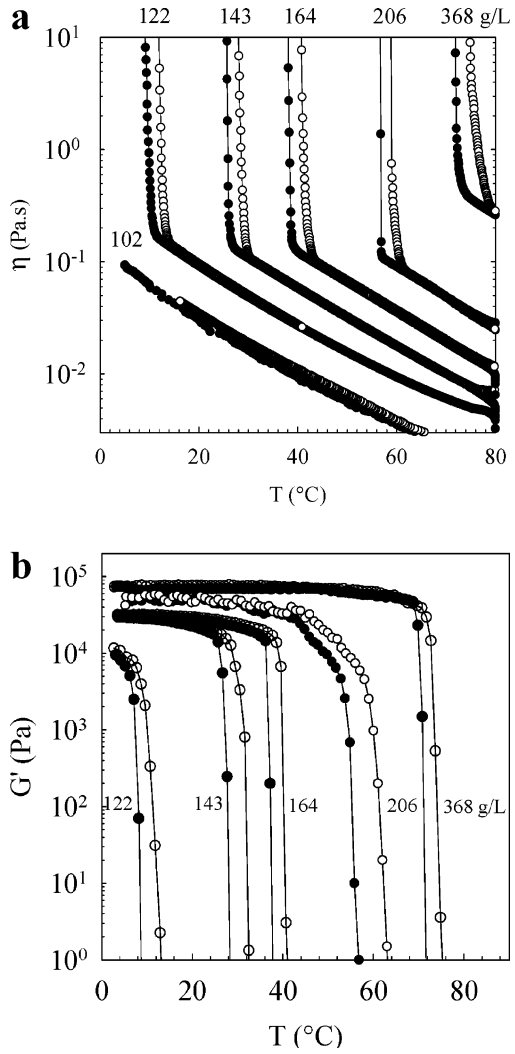

Figure 1. Temperature dependence of the viscosity (a) and the storage shear modulus (b) during cooling (filled symbols) and heating (open symbols) of micelle solutions at different concentrations. The cooling and the heating rates were 5 °C/min, and the shear stress was 10 Pa.

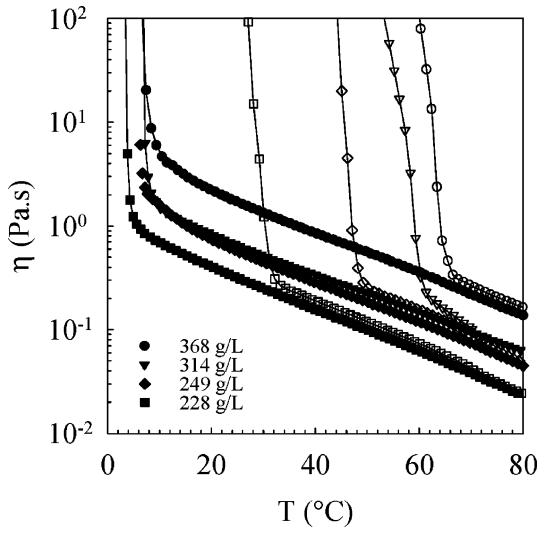

Figure 2. Temperature dependence of the viscosity of micelle solutions with added linear chains at $F = 0.1$ during cooling (filled symbols) and heating (open symbols) at different PEO concentrations. The cooling and the heating rates were 5 °C/min, and the shear stress was 10 Pa.

depended on the degree of preshearing at high temperatures. The freezing temperature decreased with increasing preshearing

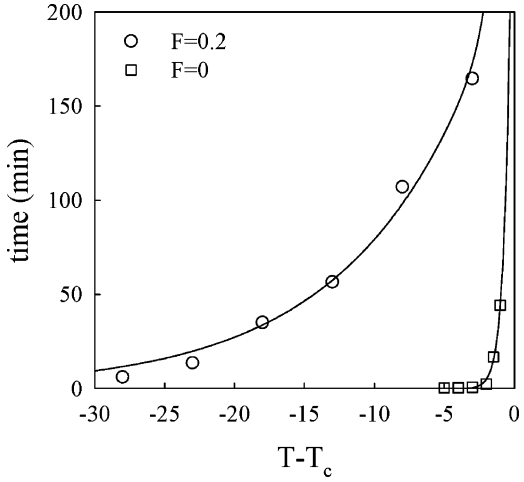

Figure 3. Freezing time as a function of $T - T_c$ for a pure micelle solution at $C = 154$ g/L (squares) and for a mixture at $F = 0.2$ at $C = 480$ g/L (triangles).

at 90 °C until after extensive preshearing (20 min at 300 s^{-1}) it reached a constant freezing temperature. It is remarkable that the freezing temperature of extensively presheared samples was approximately the same at all concentrations investigated (about 7 °C), while the melting temperature increased strongly with increasing concentration and was independent of the degree of preshearing. For a given micelle concentration, the melting temperature was lower in the presence of linear chains than for pure micelles. In the presence of linear chains at $F = 0.1$ the transition occurred at a critical viscosity that was slightly higher than for pure micelles (about 0.3 Pa·s). For pure micelles the viscosity for $T > T_c$ was the same during heating and cooling, but in the presence of linear chains it was slightly higher during heating and only became equal at high temperatures. At $F = 0.2$, similar behavior was observed (not shown), and the melting temperature decreased even more for a given micelle concentration (see below).

Kinetics of Freezing and Melting. The kinetics of freezing and melting were determined by oscillatory shear measurements as a function of time at constant temperature. The temperature was set either by rapidly cooling from 90 °C or by rapidly heating from 5 °C. Figure 3 shows that the time needed to freeze a micelle solution increased when T_c was approached. It was shown in ref 6 that it can take more than 10 h to reach steady state very close to T_c. For pure micelle solutions, the effect is only clearly visible close to T_c. However, with $F = 0.2$, the freezing rate started to slow down already 30 °C below T_c, which explains the strong hysteresis between heating and cooling ramps. At temperatures very close to T_c, it is possible to obtain the same sample in the liquid state or in the solid state for several days depending on its thermal history.

During heating a different behavior was observed. At fixed temperatures close to T_c, G' decreased first rapidly and subsequently increased more slowly back to the original value (see Figure 4). With increasing temperature, the decrease became more important, and the subsequent increase slowed down until for $T > T_c$ the system melted irreversibly. Close to T_c the system actually melted before it solidified again. These measurements indicate that a reorganization of the system occurred close to T_c. A good estimate of T_c was obtained as the temperature where the system reached the liquid state during a heating ramp of 5 °C/min.

Liquid−Solid State Diagram. The liquid−solid state diagram as a function of the temperature and the total PEO

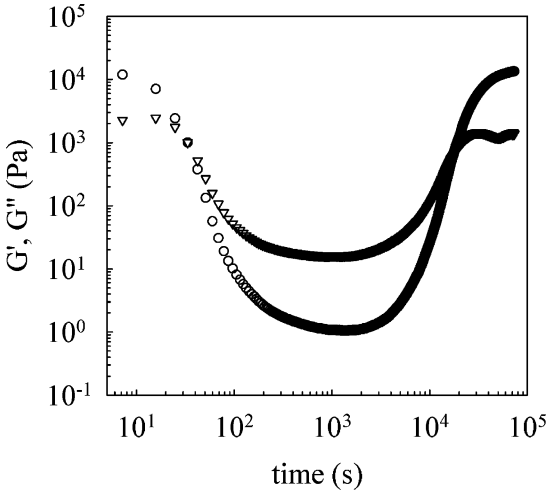

Figure 4. Transient melting for pure micelle solution at $C = 154$ g/L that was heated to a temperature just above T_c. The storage and loss moduli are represented by circles and triangles, respectively.

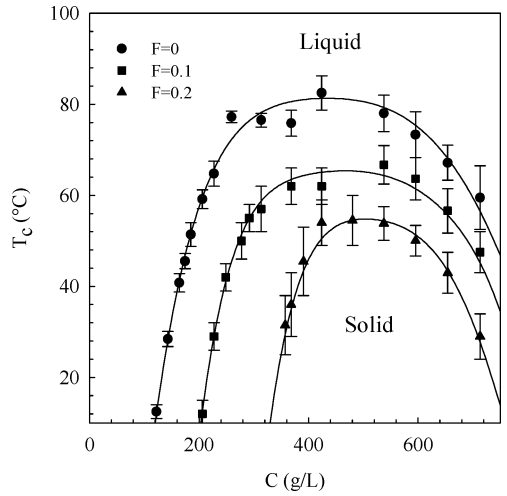

Figure 5. Liquid−solid state diagram for aqueous solutions of PEO micelles with different fractions of linear PEO chains. The error bars indicate the difference between the temperature where G' of the solid starts to decrease sharply and where the viscosity becomes equal to that of the liquid during heating at a rate of 5 °C/min. Solid lines are guides to the eye.

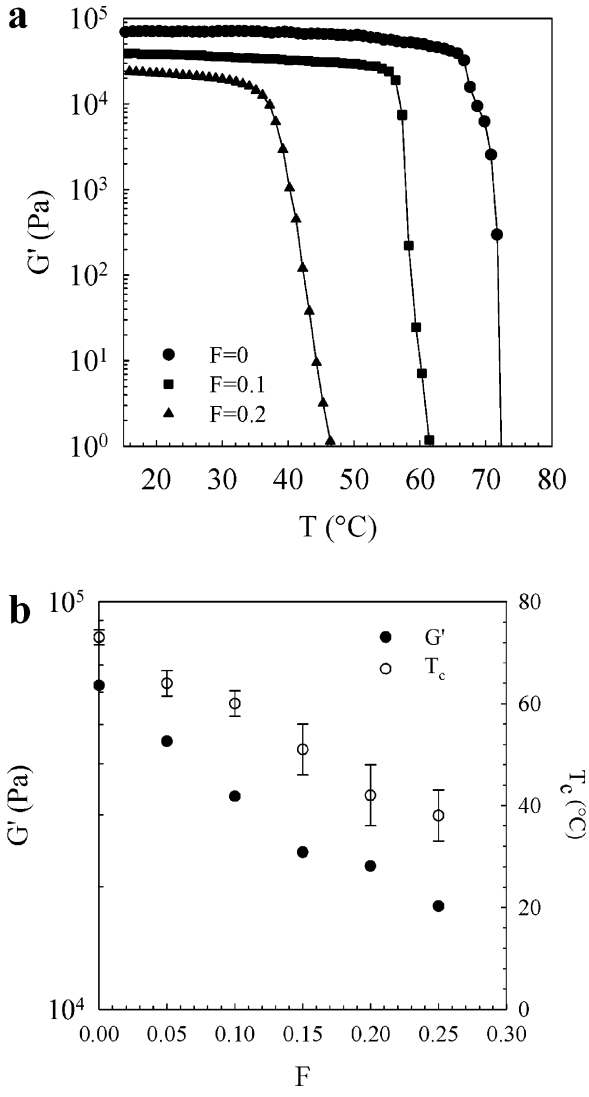

Figure 6. (a) Temperature dependence of the storage shear modulus with a fixed micelle concentration of 368 g/L and with different fractions of linear chains during heating at a rate of 5 °C/min. (b) T_c and G' at $T = T_c - 15$ °C as a function of the fraction of added linear chains.

concentration was determined for pure micelles and for $F = 0.1$ and $F = 0.2$ (see Figure 5). For pure micelles T_c increased with increasing concentration until about 230 g/L. T_c was relatively insensitive to the concentration between about 230 and 500 g/L and decreased at higher concentrations. The effect of adding linear chains was to reduce the temperature and concentration regime in which a solid was formed. If more linear chains were added, the initial increase of T_c with increasing concentration was steeper and the maximum value of T_c was smaller. The decrease of T_c occurred at approximately the same total PEO concentration, and as mentioned above, the solubility limit was about 750 g/L in all systems. The same phenomena were also reported for smaller PEO micelles by Yamazaki et al.[16] The decrease at high PEO concentrations is probably related to the fact that at high PEO concentrations the majority of water molecules is involved in hydrogen bonds with PEO.[30]

The effect of adding linear chains was studied in more detail for a constant micelle concentration of 368 g/L and thus an increasing total PEO concentration. Figure 6a shows the storage modulus during heating for several values of F. Both the storage modulus of the solid and T_c decreased with increasing F (see Figure 6b). The dependence of T_c on F appears to be linear in the limited regime that could be explored.

Continuous Flow. Continuous flow experiments were done over a range of imposed stresses at a constant micelle concentration of at 335 g/L in the absence of linear chains and for mixtures with $F = 0.1$ and $F = 0.2$. The melting temperatures of these systems were different, and in order to make a proper comparison we measured each system 40 °C below T_c. A linear increase of the strain (γ) as a function of time was observed after a transitional period with a duration that increased with decreasing stress. The shear rate ($\dot{\gamma}$) was calculated as $d\gamma/dt$ in the stationary regime.

In Figure 7, $\dot{\gamma}$ is plotted as a function of σ in a double-logarithmic representation for different values of F. Comparing the results at different F, it appears that the data are systematically shifted to lower shear stresses after addition of linear chains. Each system showed a power law dependence down to at least $\dot{\gamma} = 10^{-4}$ s^{-1}: $\dot{\gamma} \propto \sigma^{\alpha}$, with the same power law exponent within the experimental error ($\alpha = 5.3-5.5$). At lower stresses, creep was still observed, but it took longer than 24 h to obtain a constant flow rate. At high stresses a steeper increase of $\dot{\gamma}$ was found and above a critical value, σ_c, the flow rate

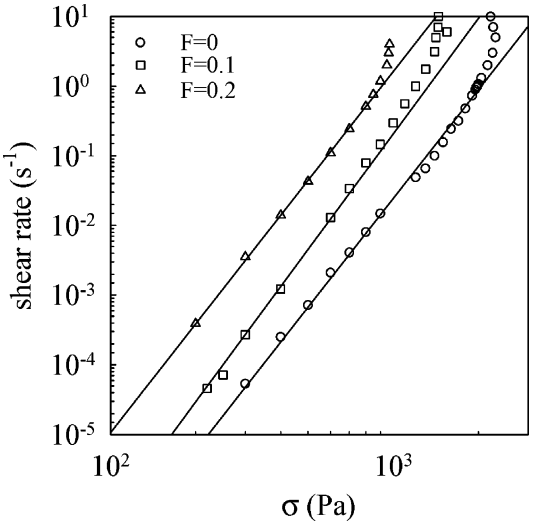

Figure 7. Double-logarithmic representation of the shear stress vs the shear rate for solutions with a fixed micelle concentration of 335 g/L and different fractions of added linear chains. The temperature for each system was 40 °C below T_c. The solid lines have slopes 5.3 for $F = 0$ and $F = 0.2$ and 5.5 for $F = 0.1$.

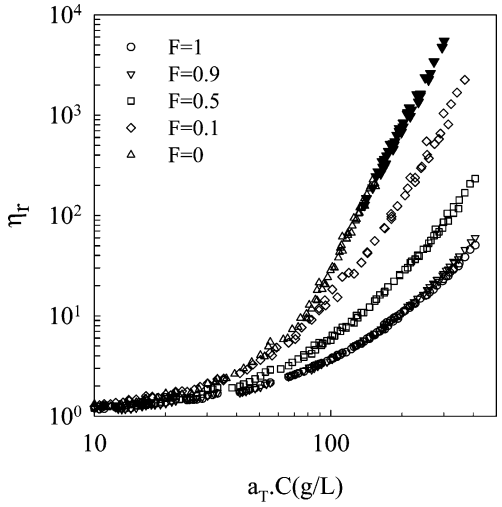

Figure 8. Master curves of the concentration dependence of the relative viscosity for linear chains, micelles, and mixtures obtained by concentration−temperature superposition with $T_{ref} = 20$ °C. The filled symbols represent data obtained by extrapolation from results at higher temperatures.

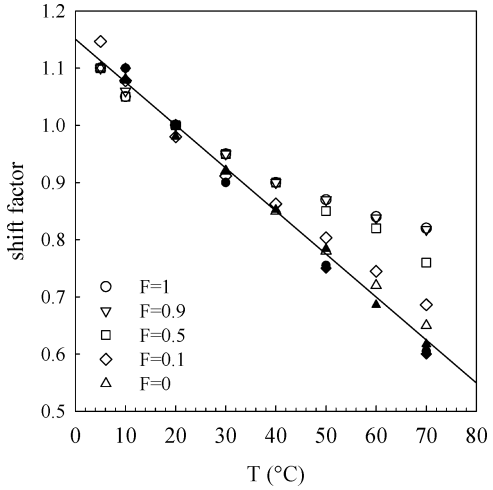

Figure 9. Temperature dependence of the shift factors used to obtain master curves of the viscosity (a_T, open symbols) and KC/I_r (b_T, filled symbols) as a function of the PEO concentration.

diverged. In separate experiments the shear stress was measured at fixed shear rates. Flow at high shear rates up to at least 50 s^{-1} occurred at a constant shear stress close to σ_c, as was reported in ref 18 for pure micelle solutions. Samples sheared at high rates became immediately solid after cessation of the flow with the same shear moduli as before the flow. Less then 1% of the deformation was recovered.

Viscosity. The viscosity of solutions of linear and micellar PEO and mixtures at $F = 0.1$, 0.5, and 0.9 was studied over a wide range of concentrations and temperatures. For systems that were solid in equilibrium the viscosity of supercooled samples was determined. For pure micelles the liquid−solid transition was too rapid to determine viscosities below T_c experimentally, but they could be estimated by extrapolation from the values at higher temperatures (see ref 6).

The viscosity normalized by that of water (η_r) increased with increasing concentration and decreasing temperature. However, the data obtained at different temperatures superimposed after multiplying C with a temperature-dependent shift factor (a_T). In Figure 8 master curves at reference temperature $T_{ref} = 20$ °C are compared for pure micelles, pure linear chains, and mixtures of micelles and linear chains. The viscosity increased more steeply with increasing PEO concentration if the fraction of linear chains was smaller. The presence of a small fraction of linear chains ($F = 0.1$) had a strong influence on the viscosity of micelle solutions, while the presence of a small fraction of micelles ($F = 0.9$) had a negligible influence on the viscosity of linear PEO solutions. The viscosity of solutions containing 50% of each component ($F = 0.5$) was closer to that of pure linear chains than pure micelles. The temperature dependence of the shift factors is shown in Figure 9. For pure micelles and the mixture at $F = 0.1$ the shift factors were the same and decreased almost linearly with increasing temperature. For linear chains the temperature dependence was weaker.

The intrinsic viscosity ($[\eta]$) was calculated from the initial concentration dependence: $[\eta] \approx 0.015$ L/g for pure linear chains and $F = 0.9$, $[\eta] \approx 0.018$ L/g for $F = 0.5$, and $[\eta] \approx 0.023$ L/g for pure micelle solutions and $F = 0.1$. One can determine an effective hard sphere radius (R_{hs}) from the expression of $[\eta]$ for hard spheres: $[\eta] = 2.5N_{av}4\pi R_{hs}^3/(3M)$. Using the molar masses determined by light scattering (see below), we obtained for the micelles $R_{hs} = 7.9$ nm at $T_{ref} = 20$ °C. R_{hs} decreased approximately linearly from 8.1 nm at 10 °C to 6.8 nm at 70 °C. For the linear chains we found that R_{hs} decreased more weakly from 2.2 nm at 10 °C to 2.0 nm at 70 °C.

Light Scattering. Static and dynamic light scattering measurements were done for solutions of pure micelles, pure linear chains, and a mixture at $F = 0.1$. The intensity obtained at different scattering wave vectors was corrected for the influence of spurious scattering using DLS as explained in the Experimental Section. The corrected intensity was independent of the scattering wave vector in the range covered by light scattering. For $C \rightarrow 0$, KC/I_r is equal to M_w^{-1}, which was found to be independent of the temperature. However, the concentration dependence of I_r depended weakly on the temperature. Again master curves could be formed by multiplying the concentration with a temperature-dependent shift factor (b_T).

Figure 10 compares master curves at $T_{ref} = 20$ °C for the pure systems and the mixture at $F = 0.1$. KC/I_r increased much more steeply for the micelles than for the linear chains, while the results obtained for the mixture were indistinguishable from those obtained for pure micelles. At high concentrations the

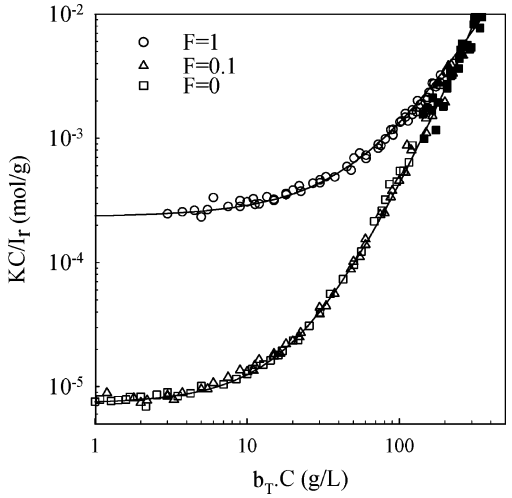

Figure 10. Master curves of the concentration dependence of KC/I_r for linear chains, micelles, and a mixture with $F = 0.1$ obtained by concentration−temperature superposition with $T_{ref} = 20$ °C. The lines are guides to the eye. The filled symbols represent data obtained for solids.

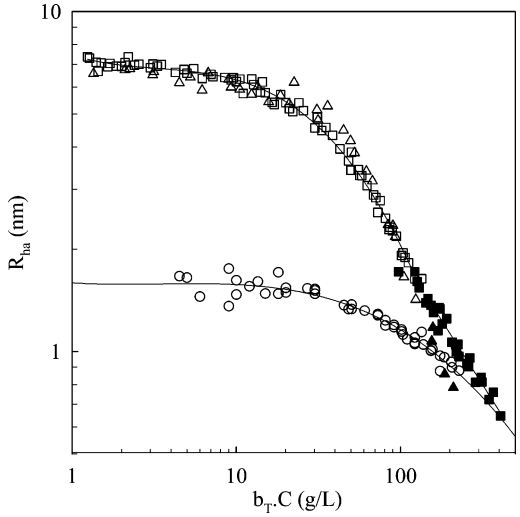

Figure 11. Master curves of the concentration dependence of the apparent hydrodynamic radius for linear chains, micelles, and a mixture with $F = 0.1$ obtained by concentration−temperature superposition with $T_{ref} = 20$ °C. The lines are guides to the eye. The filled symbols represent data obtained for solids.

values of KC/I_r became comparable for all systems. Data obtained on solid samples, indicated by filled symbols, smoothly line up with the data on liquid samples, and there is no distinct feature that signals the liquid−solid transition. The transition at different temperatures occurred at different concentrations but at approximately the same value of $KC/I_r \approx 10^{-3}$ mol/g.

The shift factors for the viscosity and the light scattering data were almost the same for pure micelle solutions and $F = 0.1$, but for pure linear chains the temperature dependence of a_T was weaker. b_T represents the decrease of the effective excluded volume interactions between PEO segments with increasing temperature. The origin of this decrease can for a large part be explained by decreasing hydration of PEO (see ref 30 and references therein).

Comparing the weight-average molar mass of the micelles ($M_w = 1.4 \times 10^5$ g/mol) with that of the precursor polymers ($M_w = 4.3 \times 10^3$ g/mol), we found that the number of arms per micelle (p) was 32 independent of the temperature. Sommer et al.[19] found at low concentrations $p = 30$ independent of the temperature from their analysis of SAXS measurements on the same system. Yamazaki et al.[31] found from light scattering $p = 26$ for smaller PEO micelles, again independent of the temperature. M_w of the mixture is dominated by the molar mass of the micelles and is thus very close to that of pure micelles.

Second virial coefficients were determined from the initial concentration dependence of KC/I_r: $A_2 = 2.5 \times 10^{-3}$ mol cm^3 g^{-2} for linear chains, and $A_2 = 2.2 \times 10^{-7}$ mol cm^3 g^{-2} for the micelles. An effective hard-sphere radius (R_{hs}) of the micelles may be calculated using the expression of A_2 for hard spheres: $A_2 = 4N_{av}4\pi R_{hs}^3/(3M_w^2)$, from which we found $R_{hs} = 7.5$ nm at $T_{ref} = 20$ °C. R_{hs} decreased from 7.7 nm at 10 °C to 6.4 nm at 70 °C. This variation was similar to that reported by Sommer et al. based on SAXS measurements.[19] It was also similar to the effective hard-sphere radii obtained from the intrinsic viscosity.

At higher concentrations the increase of KC/I_r was weaker than that of the corresponding hard spheres (see below) because the micelles can interpenetrate. At very high concentrations the micelle solution can be viewed as a concentrated solution of overlapping PEO chains in which are dispersed the alkyl cores together with a dense layer of PEO segments attached to the core.[19] If the scattering from the latter can be neglected, dense solutions of pure micelles and pure linear chains should have the same scattering intensity. Figure 10 shows that this appears to be the case for $C > 200$ g/L. The intensity scattered by the cores is small at high concentrations because they are highly ordered as was shown by SAXS experiments.[6,19] As mentioned in the Introduction, domains where the micelles have a crystalline order are formed in the solid state, but this had no effect on the osmotic compressibility of the systems, confirming that the scattering from the cores was negligible.

As discussed in the Experimental Section, the correlation functions showed a fast relaxation due to cooperative diffusion of the concentration fluctuations and an additional slow relaxation due to spurious scattering that we will ignore in the following. The cooperative diffusion coefficient was determined as a function of the PEO concentration at different temperatures. In dilute solutions D_c is related to the hydrodynamic radius (R_h) as[24]

$$D_c = \frac{kT}{6\pi\eta R_h} \tag{5}$$

If one uses eq 5 at higher concentrations, one obtains an apparent hydrodynamic radius R_{ha} that is a measure of the correlation length of the concentration fluctuations.

Master curves of the concentration dependence of R_{ha} could be obtained by concentration shifts using similar shifts factors as for KC/I (see Figure 11). The hydrodynamic radii measured at low concentrations were 1.7 nm for the linear chains and 7.2 nm for the micelles, independent of the temperature. In dilute mixtures the contribution of the linear chains at $F = 0.1$ was not observed because its relative scattering intensity was negligible. At the highest PEO concentrations D_c (and thus R_{ha}) was similar for micelles and linear chains, which is consistent with the results from static light scattering and confirms that light scattering is predominantly caused by concentration fluctuations of overlapping PEO chains. At the highest concentrations there appears to be a systematic deviation of R_{ha} at $F = 0.1$ from those of the micelles in contrast with the static light scattering results. However, it was quite difficult to determine D_c accurately at high PEO concentrations so that the deviation may not be significant.

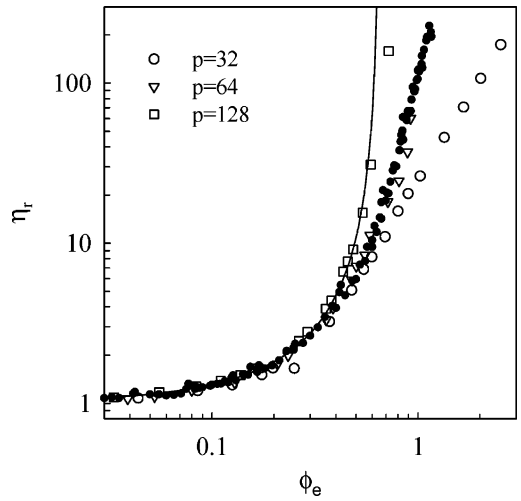

Figure 12. Dependence of the relative viscosity on the effective volume fraction for polybutadiene stars with different p and PEO micelles. The solid line represents eq 7.

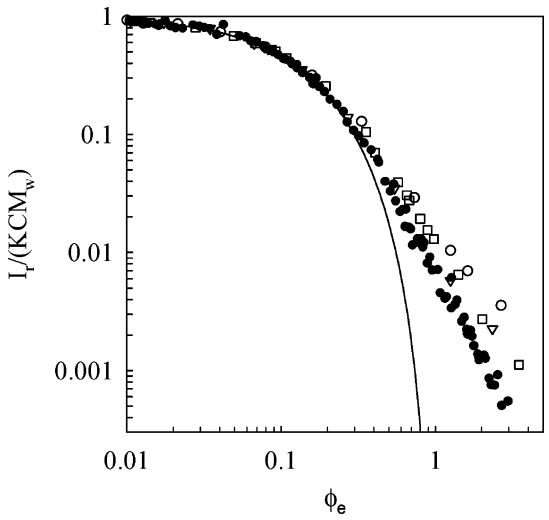

Figure 13. Dependence of $I_r/(KCM_w)$ on the effective volume fraction for polybutabiene stars with different p (open symbols) and PEO micelles (closed symbols). The symbols are as in Figure 9. The solid line represents eq 8.

Discussion

Jamming of star polymers and polymeric micelles with increasing effective volume fraction has been observed for a wide range of systems. Roovers et al. reported viscosity[3] and light scattering[32] results on solutions of polybutadiene star polymers in a good solvent. The results for three different values of aggregation numbers (32, 64, and 128) may be compared with the present results on PEO micelles. In order to facilitate the comparison, we plotted η_r (Figure 12) and the normalized scattering intensity, $I_r/(KCM_w)$ (Figure 13), as a function of the effective hard-sphere volume fraction:

$$\phi_e = (CN_{av}4\pi R_{hs}{}^3)/(3M) \tag{6}$$

Values of R_{hs} that were obtained using the intrinsic viscosity or the second virial coefficient were close, and here we have used the latter to calculate ϕ_e.

Figure 12 shows that the initial increase of η_r is similar for all systems and can be described by an equation proposed by Krieger and Dougherty for spherical particles:[33]

$$\eta_r = (1 - \phi_e/\phi_c)^{-2.5\phi_c} \tag{7}$$

with $\phi_c \approx 0.65$ the volume fraction at random close packing. For $\phi_e > 0.4$ the experimental values start to deviate because star polymers can interpenetrate.[7,10] The repulsion between the star polymers becomes weaker with decreasing p, which explains the weaker increase of the viscosity.

Roovers noted that star polymers with $p = 128$ jammed at $\phi_e \approx 0.7$ and with $p = 64$ at $\phi_e \approx 1$. The star polymers with $p = 32$ did not jam in the concentration range covered in the experiment (up to $\phi_e = 2.5$). Crystal order was not observed for any of these samples. The PEO micelles showed a steeper increase of the viscosity compared to star polymers with the same number of arms ($p = 32$) for $\phi_e > 0.6$ and resembled more closely star polymers with $p = 64$. The most likely explanation for this difference is that p increased with increasing concentration. Sommer et al.[34] found an increase of p from 30 at $\phi_e = 0.38$ (50 g/L) to 40 at $\phi_e = 0.77$ (100 g/L). In addition, it was concluded from an analysis of the crystal order of the micelles that p increased to ~100 at $\phi_e = 3$ (425 g/L).[6] Of course, an increase of p with the concentration means that the calculation of ϕ_e using eq 6 with constant M_w and R_{hs} is no longer correct at higher volume fractions. An additional contributing factor for the steeper increase could be that PEO segments are hydrated,[30] which may have an effect on the ease of interpenetration of the stars.

Figure 13 compares the dependence of $I_r/(KCM_w)$ on ϕ_e between PEO micelles and star polymers. The decrease of $I_r/(KCM_w)$ for PEO micelles was stronger than for star polymers with $p = 32$ for $\phi_e > 0.6$, and it was even slightly stronger than for star polymers with $p = 128$. The reason is most likely again that the number of arms increased with increasing PEO concentration. When the star polymers overlapped strongly ($\phi_e > 2$), $I_r/(KC)$ approached the values obtained for linear polybutadiene chains. In comparison, for the PEO micelles both $I_r/(KC)$ and D_c were close to that of linear PEO solutions for $\phi_e > 1.5$. As was noted above for the PEO micelles, there is no signature of the liquid−solid transition for star polymer solutions in the light scattering experiments.

For noninteracting hard spheres, the dependence of $I_r/(KCM_w)$ on the volume fraction is well described by an empirical equation proposed by Carnahan and Starling:[35]

$$\frac{I_r}{KCM_w} = \frac{(1-\varphi_e)^4}{1 + 4\varphi_e + 4\varphi_e{}^2 - 4\varphi_e{}^3 + \varphi_e{}^4} \tag{8}$$

indicated by the solid line in Figure 13. For star polymers, the data deviate from the hard-sphere dependence for $\phi_e > 0.3$, reflecting the softer interaction between star polymers. Likos et al.[36] proposed an effective interaction potential between star polymers from which the osmotic compressibility can be calculated. Calculated values were in close agreement with the experimental results for star polymer with $p = 128$, but the decrease with ϕ_e was somewhat weaker for $p = 32$.[37]

From this comparison, we may conclude that aqueous solutions of polymeric PEO micelles can be viewed as star polymers with an effective hard-sphere radius that increases with decreasing temperature. The increase of excluded volume interactions between the PEO segments explains why the liquid−solid transition is shifted to lower concentrations when the temperature is decreased.

A temperature-induced liquid−solid transition has also been observed for polybutadiene stars in a marginal solvent.[4] DLS showed for these systems a fast and slow relaxation mode caused

by cooperative diffusion and self-diffusion, respectively. Self-diffusion could probably be observed because the polymer stars were more polydisperse than the PEO micelles investigated here. Close to the liquid−solid transition a third slower relaxation was observed and attributed to the formation of large transient clusters. As mentioned above, the PEO micelle solutions studied here contained a small fraction of spurious scatterers, which could hide a slow mode caused by cluster formation. However, we did not observe a significant increase of the relative amplitude of the slow mode when approaching the liquid−solid transition. This means that even if clusters were formed, their contribution to the scattering intensity was very small. For polybutadiene stars the increase of the excluded volume interaction between polymer segments led to swelling of the micelles. However, for both the PEO micelles studied here and the smaller PEO micelles studied by Yamazaki[31] R_h was independent of the temperature, which shows that swelling is not actually needed for temperature-induced jamming.

Laurati et al.[11] studied frozen PEO micelles with different p using small-angle neutron scattering (SANS). Crystalline order was observed for $p = 64$ at $\phi_e \approx 1.3$ and vitrification for $p = 80$ and $p = 128$ at $\phi_e \approx 1.1$ and $\phi_e \approx 0.8$, respectively. Crystallization is predicted to occur for $p > 36$, but usually vitrification is observed instead for star polymers.[10] Note that Laurati et al. expressed their results in terms of a length scale that characterizes the interaction between star polymers which gives much smaller volume fractions than the corresponding values of ϕ_e. Computer simulations of spheres with the soft interaction potential corresponding to star polymers showed both crystallization and a strong slowing down of the dynamics.[9,13,38]

For the PEO micelles, the liquid−solid transition was abrupt and appeared to be discontinuous. Measurements at fixed temperatures close to the transition showed that the transition may be very slow, but at no temperature or concentration was a stable system formed with intermediate zero shear viscosity. The slow transition cannot be attributed to a slow exchange of arms, which was fast even in the solid state.[39] We speculate that the discontinuous transition is caused by a subtle reorganization on larger length scales, which is not reflected in a significant change of the osmotic compressibility or the structure factor. The reorganization is fast for deep quenches and becomes slow close to T_c because the driving force for the reorganization is weak. The more important slowing down in the presence of linear chains could indicate that a more substantial reorganization occurs. This could also explain the effect of preshearing on the freezing of mixtures. Apparently only after substantial preshearing is the mixture fully homogenized.

The effect of adding linear chains on the liquid−solid transition was studied earlier by Yamazaki et al.[16,17] and Stiakakis et al.[15,40,41] Yamazaki et al. studied the effect of adding linear PEO to dense solutions of PEO micelles. The difference with the systems studied here is that the molar mass of both the arms and the linear chains was about 4 times smaller so that the liquid−solid transition was shifted to higher volume fractions. They observed reduction of the freezing temperature with increasing fraction of linear chains, but they did not report melting curves or kinetics. The authors found that also in the presence of linear chains the liquid−solid transition was accompanied by the formation of domains with crystal order. We did preliminary SAXS experiments that showed the same for the mixtures of larger PEO micelles and linear chains studied here. It was suggested by Yamazaki et al. that a fraction of the linear chains cannot penetrate the corona, which would weaken the excluded volume interaction between the micelles. The same authors showed that the weakening effect was stronger if the added linear chains were larger. We tested the effect of adding unfunctionalized PEO with different molar masses between 0.35 and 20 kg/mol and confirmed that the effect increases with increasing molar mass.

Stiakakis et al.[15,40,41] investigated the effect of adding linear chains to dense solutions of covalent star polymers. In refs 15 and 41 they reported a study of mixtures of polybutadiene stars and linear chains in an athermal solvent, varying the molar mass of the linear chains from much smaller to much larger than the arm molar mass. A decrease of G' was observed for the solid with increasing concentration or molar mass of the linear chains, and the system melted at a critical concentration or molar mass of the linear chains. Upon further increase of the molar mass or the concentration, the viscosity decreased. This effect was attributed to weakening of the repulsion between the stars due to depletion of the linear chains.

In ref 40 mixtures of star and linear polymers were studied in a marginal solvent for which the jamming of the stars could be induced by increasing the temperature which increased the excluded volume of the polymers. This situation is analogous to the one studied here where the excluded volume increased with decreasing temperature. When large chains were added, the solid weakened or even melted similarly to the observations in good solvents. However, adding linear chains much smaller than the arms led to stronger solids because very small chains can easily penetrate the stars and thus improve the solvent quality for the stars. For the system studied here we did not observe a strengthening effect even when using PEO chains with $M_w = 350$ g/mol, but the weakening effect was much smaller.

From the measurements reported here we may conclude that melting by increasing the temperature is simply caused by a decrease of the solvent quality for PEO and thus of the effective volume fraction of the micelles. Such a conclusion cannot as easily be drawn for the effect of adding linear chains because the osmotic compressibility of the system did not decrease significantly when linear chains were added. The reason is that it is dominated by the osmotic compressibility of the overlapping PEO segments. In order to observe the effect of adding linear chains on the interaction between the micelles, one needs to detect the scattering from the micellar cores, which can be done, in principle, with SANS or SAXS.

On the other hand, adding linear chains significantly reduced the viscosity of the liquids and the shear modulus of the solids, which indicates a reduction of the repulsion between the micelles.[42] As a consequence, when applying the same shear stress on jammed micelle solutions they flowed faster after addition of linear chains. Linear chains do not freely interpenetrate the micelles, but neither will they be completely excluded.[16] They are most likely situated at the interfaces between micelles so that excluded volume interaction between segments of adjacent micelles will be partially screened. Screening also occurs within the corona and may lead to shrinking of the micelles if the corona chains are sufficiently large.[40] However, the linear chains cannot be distributed homogeneously over all interfaces between micelles as this would imply stretching of the chains. Depletion effects are therefore expected.[41] It would be of interest to localize precisely the linear chains in the close-packed micelle solution. It is possible that the equilibrium distribution of the linear chains in the system varies with the temperature. The slow kinetics, the strong hysteresis, and the effect of preshear are perhaps emanations of nonequilibrium distributions of the linear chains.

Summary

Aqueous solutions of polymeric micelles formed by hydrophobically end-capped PEO show a discontinuous liquid−solid transition at a critical value of the effective volume fraction that can be increased either by increasing the PEO concentration or by decreasing the temperature. The rate of the transition decreases close to the transition temperature. The viscosity and osmotic compressibility at the transition point are independent of the temperature and the PEO concentration. Addition of nonfunctionalized linear PEO chains leads to a decrease of the critical transition temperature and the shear modulus of the solid. This effect is probably caused by screening of the excluded volume interaction between micelles. Transient melting, hysteresis, and effects of preshear are observed during cooling and heating that are probably related to slow structural rearrangement of the system.

Adding a small amount of linear chains has a strong influence on the rheology but no significant effect on the light scattering intensity or the cooperative diffusion coefficient. The amplitude and the relaxation of concentration fluctuations are dominated by the osmotic compressibility of the PEO segment of overlapping chains.

Acknowledgment. This work has been financially supported by a grant from the program "Contrat Etat-Région n° 18026 Polymères-Plastique" of the French Ministry for National Education and Research and the Région des Pays de la Loire, and a grant from the Marie-Curie program (MRTN-CT-2003-504712) of the European Union.

References and Notes

(1) Hamley, I. W. In *The Physics of Block Copolymers*; Hamley, I. W., Ed.; Oxford University Press: Oxford, 1998; pp 131−220.
(2) Lund, R.; Willner, L.; Richter, D.; Dormidontova, E. E. *Macromolecules* **2006**, *39*, 4566−4575.
(3) Roovers, J. *Macromolecules* **1994**, *27*, 5359−5364.
(4) Loppinet, B.; Stiakakis, E.; Vlassopoulos, D.; Fytas, G.; Roovers, J. *Macromolecules* **2001**, *34*, 8216−8223.
(5) Wanatabe, H. *Acta Polym.* **1997**, *48*, 215−233.
(6) Nicolai, T.; Laflèche, F.; Gibaud, A. *Macromolecules* **2004**, *37*, 8066−8071.
(7) Vlassopoulos, D. *J. Polym. Sci., Part B: Polym. Phys.* **2004**, *42*, 2931−2941.
(8) Watzlawek, M.; Likos, C. N.; Lowen, H. *Phys. Rev. Lett.* **1999**, *82*, 5289−5292.
(9) Foffi, G.; Sciortino, F.; Tartaglia, P.; Zaccharelli, E.; Lo Verso, F.; L.; Reatto, L.; Dawson, K. A.; Likos, C. N. *Phys. Rev. Lett.* **2003**, *90*, 238301.
(10) Likos, C. N. *Soft Matter* **2006**, *2*, 478−498.
(11) Laurati, M.; Stellbrink, J.; Lund, R.; Willner, L.; Richter, D.; Zaccarelli, E. *Phys. Rev. Lett.* **2005**, *94*.
(12) Likos, C. N.; Löwen, H.; Poppe, A.; Willner, L.; Roovers, J.; Cubitt, B.; Richter, D. *Phys. Rev. E* **1998**, *58*, 6299−6307.
(13) Rissanou, A.; Yiannourakou, M.; Economou, I. G.; Bitsanis, I. A. *J. Chem. Phys.* **2006**, *124*, 044905.
(14) Watanabe, H.; Kotaka, T. *J. Rheol.* **1983**, *27*, 223−240.
(15) Stiakakis, E.; Vlassopoulos, D.; Likos, C. N.; Roovers, J.; Meier, G. *Phys. Rev. Lett.* **2002**, *89*, 208302−208301.
(16) Yamazaki, R.; Nose, T. *Polymer* **2003**, *44*, 6501−6511.
(17) Yamazaki, R.; Numasawa, N.; Nose, T. *Polymer* **2004**, *45*, 6227−6234.
(18) Nicolai, T.; Benyahia, L. *Macromolecules* **2005**, *38*, 9794−9802.
(19) Sommer, C.; Pedersen, J. S.; Stein, P. C. *J. Phys. Chem. B* **2004**, *108*, 6242−6249.
(20) Brown, W. *Light Scattering. Principles and Developments*; Clarendon Press: Oxford, 1996.
(21) Higgins, J. S.; Benoit, H. C. *Polymers and Neutron Scattering*; Clarendon Press: Oxford, 1994.
(22) Venohr, H.; Fraaije, V.; Strunk, H.; Borchard, W. *Eur. Polym. J.* **1998**, *34*, 723−732.
(23) Devanand, K.; Seler, J. C. *Macromolecules* **1991**, *24*, 5943−5947.
(24) Berne, B.; Percora, R. *Dynamic Light Scattering*; Wiley: New York, 1976.
(25) Brown, W., Ed. *Dynamic Light Scattering. The Method and Some Applications*; Clarendon Press: Oxford, 1993.
(26) Duval, M. *Macromolecules* **2000**, *33*, 7862−7867.
(27) Hammouda, B.; Ho, D. L.; Kline, S. *Macromolecules* **2004**, *37*, 6932−6937.
(28) Kinugasa, S.; Nakahara, H.; Fudagawa, N.; Koga, Y. *Macromolecules* **1994**, *27*, 6889−6892.
(29) Chassenieux, C.; Nicolai, T.; Durand, D. *Macromolecules* **1997**, *30*, 4952−4958.
(30) Dormidontova, E. E. *Macromolecules* **2002**, *35*, 987−1001.
(31) Yamazaki, R.; Inomata, K.; Nose, T. *Polymer* **2002**, *43*, 3647−3652.
(32) Roovers, J.; Toporowski, P. M.; Douglas, J. *Macromolecules* **1995**, *28*, 7064−7070.
(33) Krieger, I. M. *Adv. Colloid Interface Sci.* **1972**, *3*, 111.
(34) Sommer, C.; Pederson, J. S.; Garamus, V. M. *Langmuir* **2005**, *21*, 2137−2149.
(35) Carnahan, N. F.; Starling, K. E. *J. Chem. Phys.* **1969**, *51*, 635−636.
(36) Likos, C. N.; Lowen, H.; Watzlawek, M.; Abbas, B.; Jucknischke, O.; Allgaier, J.; Richter, D. *Phys. Rev. lett.* **1998**, *20*, 4450−4453.
(37) Zacharelli, E., private communication.
(38) Lo Verso, F.; Tau, M.; Reatto, L. *J. Phys.: Condens. Matter* **2003**, *15*, 1505−1520.
(39) Laflèche, F.; Durand, D.; Nicolai, T. *Macromolecules* **2003**, *36*, 1331−1340.
(40) Stiakakis, E.; Vlassopoulos, D.; Roovers, J. *Langmuir* **2003**, *19*, 6645−6649.
(41) Stiakakis, E.; Petekidis, G.; Vlassopoulos, D.; Likos, C. N.; Iatrou, H.; Hadjichristidis, N.; Roovers, J. *Europhys. Lett.* **2005**, *72*, 664−670.
(42) Buitenhuis, J.; Forster, S. *J. Chem. Phys.* **1997**, *107*, 262−272.

MA070263E